Quest: Journal of Geometry, Mathematical and Quantum Physics
e-ISSN: 3064-7282 Vol.3 Issue 3|2026

A Theoretical and Experimental Comparative Study of Proton Energy Loss in Various Elements and the Effects of Density Polarization and Shell Binding

Abdullah Z. Nuri
Ministry of Higher Education and Scientific Research, Tikrit University,
College of Education - Tuz Khurmatu, Iraq
Email: abdullah.zahem.tuz@tu.edu.iq

Abstract: This research presents a comprehensive physical and computational model of the specific energy loss mechanism of incident protons over an energy range of 10 MeV to 1000 MeV in three elements with different compositions and atomic numbers: silicon (Si), copper (Cu), and gold (Au). This model employs a modified Beth-Bloch equation that considers the effects of density and shell structure. The dynamic characteristics of the incident proton's kinetics and its susceptibility to polarization and atomic bonding (shell structure) were investigated. The computational results and comparative analyses of the extracted computational tables demonstrate the crucial role of shell correction in suppressing low energies to prevent spikes in the theoretical calculations. This is achieved by considering the density Sternheimer correction limit as an electrostatic shielding barrier that ensures the stability of the radiation curve at high energies. The study adopted the precise log_10 βγ quantity to enhance the systems used in radiological medical planning and the development of nuclear shielding technologies, with results that closely match experimental reality.

Keywords: Beth-Bloch equation, Density effect correction, Relative Lorentz coefficient, Shell correction, Stopping power

Introduction

The penetration of charged particles into a material is considered the cornerstone upon which radiation detection applications, space shield design, and protection against nuclear radiation are built, in addition to medical radiation applications such as proton therapy [1-2]. When a heavy charged particle with mass $M \gg m_e$ such as a nucleus or a proton—penetrates a medium, it gradually loses its initial incident kinetic energy as a result of a series of inelastic Coulomb collisions it undergoes with the atomic electrons of the target or absorbing material [3-4].

The amount of energy lost by the particle per unit distance, denoted by $-dE/dx$, is known as the Coulomb stopping power or collision stopping power. At high energies below a few gigaelectronvolts GeV, electronic ionization and excitation processes overwhelmingly dominate the energy loss mechanisms. At the same time, the energy loss resulting from electromagnetic interaction with the nucleus remains significant only in extremely low energy ranges [5-6].

The description of the energy loss phenomenon has passed through multiple physical stages, starting from the classical theory presented by Niels Bohr in 1913, reaching the precise quantum theory formulated by Hans Bethe and Felix Bloch. Nevertheless, the complex nature of electronic binding

within multi-electron atoms and the polarization effects in dense solids necessitated the introduction of highly precise physical corrections to enable the theoretical formula to accurately predict experimental results [7-8].

In our present study, three elements with varying densities and atomic structures were selected to cover a broad spectrum of radiation-matter interaction levels [9-10]:

1. Silicon (Si): This element represents a semiconductor and low-density medium. It serves as the primary material in the design and fabrication of solid-state detectors, as well as in radiation loss calculations and ionization dose assessments within microelectronic chips.
2. Copper (Cu): This element represents a metallic medium with intermediate density and atomic number. It is extensively used as a nuclear radiation shield and in the essential structural components of particle accelerators.
3. Gold (Au): This element represents a heavy, high-density, and high-atomic-number metallic medium. It is utilized in ultra-high-precision micro-applications such as advanced radiation shielding for protecting sensors, as a target material for high-energy collisions in particle production, and as a coating for resonant cavities and conductors to prevent oxidation while ensuring and enhancing the efficiency of electrical signal transmission.

The aim of this study is to present an integrated physical and computational modeling of the energy loss mechanism for incident protons within an energy range extending from 10 MeV to 1000 MeV in elements with varying densities and atomic numbers (Silicon, Copper, and Gold), by applying the modified Bethe-Bloch formula. In addition, it takes into account the dynamic effect of atomic shell corrections at low energies and Sternheimer's density effect at high energies, aiming to provide precise calculations that contribute to enhancing medical radiation therapy planning systems and developing nuclear shielding techniques with an efficiency that closely matches experimental reality [11-12].

2. Mathematical Formulation of the Relativistic Bethe-Bloch Equation

The modern quantum formulation for calculating the radiative (and ionization) energy loss of heavy charged particles relies on the First-Order Born Approximation. In this treatment, the interaction is treated as a momentum transfer from the fast-moving incident particle particularly at high energies to the stationary electrons of the absorbing medium [13-14].

The modified Bethe-Bloch equation, incorporating all standard physical corrections, is written as follows [5-10]:

$$-\frac{dE}{dx} = 2\pi N_a r_e^2 m_e c^2 \rho \frac{Zz^2}{A\beta^2}\left(\ln\left(\frac{2 m_e c^2 \beta^2 \gamma^2 W_{max}}{I^2}\right) - 2\beta^2 - \delta - \frac{2C}{Z}\right) \quad (1)$$

The physical constants can be expressed through a constant factor k, which simplifies numerical calculations. The value of this constant is equal to:

$$k = 2\pi N_a r_e^2 m_e c^2 = 0.1535\ MeV.cm^2/g$$

The equation will then take the form:

$$-\frac{dE}{dx} = k\rho \frac{Zz^2}{A\beta^2}\left(\ln\left(\frac{2 m_e c^2 \beta^2 \gamma^2 W_{max}}{I^2}\right) - 2\beta^2 - \delta - \frac{2C}{Z}\right) \quad (2)$$

Below is a detailed definition of the physical and universal constants and parameters [15-16]:

N_a : Avogadro's number $6.02214 \times 10^{23} mol^{-1}$.
r_e^2 : Classical electron radius $2.8179 \times 10^{-13}\ cm$.
$m_e c^2$: Electron rest mass energy $0.5109989\ MeV$.
ρ :Mass density of the medium Measured in $\frac{g}{cm^3}$.
Z : Atomic number of the target material Represents the number of electrons per atom.

A : Atomic weight of the target material Measured in g/mol.
z : Charge of the incident particle Measured in units of the elementary charge e (for a proton, z = 1).

β :Relative velocity of the particle.
γ : Relativistic Lorentz factor.
I : Mean excitation potential of the material Represents the logarithmic average of the electronic excitation and ionization frequencies in the atom, measured in electronvolts eV.
W_{max} :Maximum energy transfer in a single collision Calculated precisely using relativistic collision mechanics.

δ :Sternheimer density effect correction: Accounts for the polarization of the material medium at high energies.

C :Shell correction Accounts for the non-mobility or rigidity of inner orbital electrons at low energies.

3. Rigorous Physical Analysis of Corrections and Kinematic Parameters

3.1 Calculation of Maximum Energy Transfer W_{max}

In a head-on collision between an incident particle of rest mass M and kinetic energy E_k, and a stationary electron of rest massm_e, the maximum kinetic energy that the electron can acquire is given by the exact relativistic relation [4-5]:

$$W_{max} = \frac{2\, m_e c^2 \eta^2}{1 + 2s\sqrt{1+\eta^2} + s^2} \qquad (3)$$

Where $\eta = \beta\gamma = \frac{p}{Mc}$, p is the momentum of the incident particle, and $s = \frac{m_e}{M}$ is the ratio of the electron mass to the incident particle mass. In the case of protons as incident particles, their rest mass is equal to $M_p = 938.272013\ MeV$, while the electron rest mass is $m_e = 0.5109989\ MeV$; consequently [5-16]:

$$s = \frac{0.5109989}{938.272013} = 5.44616 \times 10^{-4}$$

Since $s \ll 1$ (substantially smaller than unity), the terms in the denominator approach unity. Therefore, at non-ultra-relativistic energies, the equation simplifies to:

$$W_{max} = 2\, m_e c^2 \gamma^2 \beta^2 \qquad (4)$$

3.2 Mean Excitation Potential (I) and its Dependence on Atomic Number (Z)

The mean excitation (or ionization) potential, I is considered the fundamental material property that resists energy loss. Geometrically, it reflects the binding strength of electrons to the nucleus across various atomic shells. Due to the extreme complexity of theoretical calculations for the mean excitation potential, Sternheimer et al. formulated empirical equations relating the mean excitation potential I to the atomic number Z for pure elements[17-18]:

$$\frac{I}{Z} = \begin{cases} 12 + \frac{7}{Z} eV \ \ for\ Z < 13 \\ 9.76 + 58.8\, Z^{-1.19} eV \ \ for\ Z \geq 13 \end{cases} \qquad (5)$$

3.3 Modeling the Sternheimer Density Effect Correction

As the velocity of the incident particle increases toward relativistic values approaching the speed of light its electric field undergoes Lorentz contraction longitudinally and expands significantly in the transverse direction. This expansion increases the range of the Coulomb interaction with atoms far

from the particle's trajectory in dense materials (solids and liquids), as well as in high-pressure gases.

In this case, the electric field of the particle polarizes the electrons of nearby atoms. This polarization acts as a shielding effect (screening effect) that reduces the effective electric field strength experienced by distant electrons, thereby causing a reduction in the actual rate of energy loss compared to the classical theoretical Bethe-Bloch formulation.

This shielding is accurately modeled using standard Sternheimer equations based on the kinematic variable X, which is given by the following relation [18]:

$$X = \log_{10} \beta\gamma \qquad (6)$$

And the value of the Sternheimer density effect correction, δ is given by the following piecewise equation:

$$\delta = \begin{cases} 0 & \text{if } X < X_0 \\ 4.6052\,X + C_0 + a\,(X_1 - X)^m & \text{if } X_0 \le X < X_1 \\ 4.6052\,X + C_0 & \text{if } X \ge X_1 \end{cases} \qquad (7)$$

Where the value of the constant parameter C_0 is determined physically through the material's plasma frequency relation $h\nu_p$:

$$C_0 = -\left(2\ln\left(\frac{I}{h\nu_p}\right) + 1\right) \qquad (8)$$

And the plasma frequency of the medium, $(h\nu_p)$ is calculated using the equation:

$$\nu_p = \sqrt{\frac{N_e e^2}{\pi m_e}} = \sqrt{80.617 \times 10^6\ cm^3\ N_e}\ Hz \qquad (9)$$

Where $N_e = \frac{N_a \rho\, Z}{A}$ is the electron volume density in the attenuating medium.

3.4 Modeling the Atomic Shell Correction (C)

When the velocity of the incident particle is low enough to approach or drop below the orbital velocity of bound electrons in the inner atomic shells particularly the K and L shells the inner electrons can no longer absorb energy as freely bound particles. This reduces the stopping power compared to theoretical predictions.

To account for this effect, the atomic shell correction term C is introduced. The mathematical expression for the shell correction is empirically derived as a function depending on the parameters η and the mean excitation potential I, as follows [5]:

$$C_{(I,\eta)} = (0.422377\,\eta^{-2} + 0.0304043\,\eta^{-4} - 0.00038106\,\eta^{-6})\,10^{-6}I^2 + (3.850190\,\eta^{-2} - 0.1667989\,\eta^{-4} + 0.00157955\,\eta^{-6})10^{-9}I^3 \qquad (10)$$

As previously noted, $\eta = \beta\gamma$ and the value of I in this equation is substituted in units of electronvolts (eV). To carry out accurate mathematical calculations, reference must be made to the constants in Table (1) to achieve the highest degree of agreement with experimental results.

Table (1): Physical constants and Sternheimer density correction parameters for the three selected elements [5]:

Physical Constant	Silicon (Si)	Copper (Cu)	Gold (Au)
Effective Atomic Number: (Z)	14	29	79
Effective Atomic Weight: A (g/ mol)	28.086	63.546	196.967
Density: ρ (g/cm^3)	2.33	8.96	19.32
Mean Excitation Potential :I (eV)	173	322	790

Density correction constant: $(-C_\circ)$	4.435	4.419	5.57
Coefficient: (a)	0.1492	0.1434	0.0976
Coefficient: (m)	3.254	2.904	3.11
Lower energy limit$(X_\circ)$	0.2014	−0.0254	0.2021
Upper energy limit X_1	2.871	3.279	3.70

4. Mathematical Calculations for Proton Energy Loss

We will now perform the mathematical treatment and precise numerical calculations for a proton with a kinetic energy E_k ranging from $10\text{MeV}\ to\ 1000\text{MeV}$ as it passes through silicon, copper, and gold.

A primary priority in our calculations is to determine the relativistic kinematic quantities (η, β, γ) using the rest energy of the proton, $E_0 = M_p c^2 = 938.272\ MeV$. The total energy of the proton, E is given by $E = E_k + E_0$, and the relativistic Lorentz factor, γ is determined from the relation: $\gamma = \frac{1}{\sqrt{1-\beta^2}}$, and the square of the relative velocity β^2 was obtained from the relation: $\beta^2 = 1 - \frac{1}{\gamma^2}$ and the square of the kinematic parameter, η^2 was obtained from the relation: $\eta^2 = \beta^2\gamma^2$ then, the maximum energy transfer, W_{max} was calculated from Equation (3) using the exact formula that depends on the parameter $s = 5.44616 \times 10^{-4}$ [15-16].

When determining the value of the Sternheimer density effect correction, δ it must be taken into account that as the proton moves at very high velocities through a dense material medium, its electric field undergoes relativistic deformation known as Lorentz contraction causing it to extend transversely over large distances. This transverse expansion increases the probability of interaction with atomic electrons located far from the particle's trajectory.

In reality, however, the atoms of the material medium respond to this electric field through electric polarization, where nearby atomic electrons act as a shielding screen (shielding effect) that screens distant electrons from the full field of the incident particle. This shielding reduces the rate of energy loss of the particle compared to the predictions of the classical Bethe-Bloch equation. Without incorporating the density correction δ the theoretically calculated stopping power values (dE/dx) at high energies would be significantly higher than the actual experimental values [17].

To achieve the highest degree of accuracy in calculating the specific radiative loss (or specific energy loss), the mathematical Sternheimer parameterization model was adopted to calculate the density effect correction parameter (δ). A dynamic algorithmic logic was built within the computational workspace using nested-IF functions to partition the motion of protons through various media into three kinematic regimes according to Equation (7), based on the relative kinematic variable according to Equation (6), which can be formulated as follows [10-12]:

$$X = \log_{10}\left(\sqrt{\eta^2}\right) \qquad (11)$$

This software tab ensures that the correction value is automatically activated in its exact form as soon as the particle exceeds the critical polarization limits (X_0) and reaches saturation (X_1) for each element separately based on its experimental physical constants taken from the standard Sternheimer tables (a, m, C_0) and listed in Table No. (1) [5].

In the final term of the Bethe-Bloch equation, we evaluated the shell correction value C using Relation (10). Utilizing both the atomic shell correction term (C) and the density effect correction (δ) in the Bethe equation guarantees theoretical precision in stopping power calculations, aligning them with experimental results across broad energy ranges of the incident particle.

We also calculate the percentage deviation of the theoretical values from the experimental values for each energy point using the following formula:

$$\text{Percentage Deviation \%} = \left|\frac{\text{Theory} - \text{Experiment}}{\text{Experiment}}\right| \times 100 \qquad (12)$$

5. Results and Discussion

The comparison and numerical results presented in Tables (2,3,4) show a high-precision physical agreement between the mathematical values derived from the Beth-Bloch equation developed with the universal experimental values presented in the book of experimental results by Janni's [11]. A software algorithm, based on the preceding detailed steps, was written to calculate the stopping power of protons at kinetic energies ranging from 10 MeV to 1000 MeV. Table (2) shows that for silicon, the stopping power of protons at low energies (10 MeV) reaches its highest value of (34.55392 MeV.cm^2/g), deviating by 0.69% from the experimental stopping power. This is physically attributed to the fact that a slower-moving particle spends more time passing near atomic electrons, significantly increasing the probability of Coulomb energy transfer. Simultaneously, at the same energy, we observe the shell correction value (1.293227), which acts as a quantum brake, preventing overestimation of losses due to the proton's low velocity compared to the orbital velocity of electrons in the inner silicon shells. As the kinetic energy of the incident proton increases, the stopping power gradually decreases according to the relationship... The inverse with the square of the velocity ($1/v^2$) until it reaches its lowest value (1.8077 MeV.cm^2/g) at an energy of ($1000\ MeV$) and with a deviation of 0.4341% from the experimental stopping power. This is known as the range of particles with the lowest ionization [5-11], In this high energy range, the shell limit correction completely disappears to approach zero (0.009974) for the large particle velocity compared to the atomic orbitals, while the density correction limit (δ) begins to be actively active or exceeds the threshold limit at an energy of ($900\ MeV$) with a precise value of (0.140529). This is due to the polarization caused by the solid silicon medium, which blocks part of the extended electric field of the high-energy proton, i.e., the relatively fast one. This leads to a reduction and stabilization of the stopping power at these limits without the occurrence of false spikes.

Table (2): shows the calculations for attenuation and energy loss of protons in the semiconductor element silicon:

Proton kinetic energy (MeV)	Square of the proton's relativistic velocity β^2	Combined relativistic kinematic coefficient η^2	Maximum energy transfer in a single collision W_{max} (eV)	Correction value for the effect of the atomic shell C(unitless)	Density effect correction value δ(unitless)	Stopping Power (MeV. cm	Stopping Power (MeV. cm Experiment [11]	Percentage Deviation %
10	0.02098	0.021429	21876.68	1.293227	0	34.55392	34.794	0.69
50	0.098627	0.109419	111697.5	0.299131	0	9.875074	9.8896	0.1468
100	0.183351	0.224517	229179.4	0.14573	0	5.851391	5.8562	0.0821
150	0.256668	0.345295	352444.9	0.094654	0	4.395494	4.3981	0.0592
200	0.320538	0.471752	481493	0.069232	0	3.639259	3.6409	0.0450
300	0.42585	0.741705	756932.5	0.043997	0	2.864931	2.8658	0.0303
400	0.508449	1.034376	1055490	0.031534	0	2.475172	2.4757	0.0213
500	0.574426	1.349766	1377158	0.024159	0	2.244443	2.2442	0.0108
600	0.627959	1.687873	1721927	0.019316	0	2.094694	2.0933	0.0666
700	0.671991	2.048699	2089790	0.015912	0	1.991645	1.9889	0.1380
800	0.708645	2.432242	2480740	0.013401	0	1.917861	1.9137	0.2174
900	0.739482	2.838504	2894767	0.011482	0.140529	1.848968	1.8579	0.4807
1000	0.76567	3.267484	3331864	0.009974	0.15016	1.807718	1.8156	0.4341

Table (3) represents the results of values and calculations of the behavior of the proton absorbed by the copper element. The value of the stopping power of the proton at low energy (10 MeV) is equal to (27.0859 MeV.cm^2/g), with a deviation of 0.1368% from the experimental value. We note that this value is significantly lower than its counterpart in the silicon element, despite the increase in the number of electrons in the atom of the copper element. The direct explanation for this

phenomenon lies in the quantum structure of the atom, where copper electrons are more strongly bound to the nucleus due to the positive charge $(+29e)$ [7-8]. We observe a sharp increase in the shell correction limit, which equals 4.124163. This high value of the shell correction limit physically means that the inner electrons become unable to absorb the low-speed, low-energy proton. Therefore, the shell limit plays a crucial role in reducing the overall stopping power at low energies. As the proton energy increases within the relative range, the stopping power of the proton gradually decreases until it reaches its minimum value $(1.52173\text{MeVcm}^2/\text{g})$ at the highest energy value $(1000\ MeV)$. With increasing energies, we observe the activation of the density effect Sternheimer limit in copper at an earlier and more pronounced time. This limit begins to rise at 400 MeV with a value of 0.096431 and its value gradually increases with increasing energy until it reaches 0.323632 at 1000 MeV, at which point the stopping power decreases. To values of 1.52173 and a deviation of 2.00089%. This value of deviation was recorded as the highest value for the three elements. The early activity and increasing effect of the density correction limit is due to the high volumetric electron density of copper resulting from the proximity of the copper element and its metallic bonding. This makes copper provide a rich environment for electrical polarization, which in turn blocks the transverse field of the incident proton and works to restrict radioactive loss very effectively [17].

Table (3): shows the calculations for attenuation and energy loss of protons in the medium-density metallic element (copper):

Proton kinetic energy (MeV)	Square of the proton's relativistic velocity β^2	Combined relativistic kinematic coefficient η^2	Maximum energy transfer in a single collision W_{max} (eV)	Correction value for the effect of the atomic shell C(unitless)	Density effect correction value δ(unitless)	Stopping Power (MeV. cm	Stopping Power (MeV. cm Experiment [11]	Percentage Deviation %
10	0.02098	0.021429	21876.68	4.124163	0	27.0859	27.123	0.1368
50	0.098627	0.109419	111697.5	1.383295	0	8.101663	8.1076	0.07323
100	0.183351	0.224517	229179.4	0.720824	0	4.859909	4.8636	0.07588
150	0.256668	0.345295	352444.9	0.479156	0	3.671156	3.6746	0.09373
200	0.320538	0.471752	481493	0.354582	0	3.049998	3.053	0.09833
300	0.42585	0.741705	756932.5	0.227993	0	2.411376	2.4138	0.10041
400	0.508449	1.034376	1055490	0.164363	0.096431	2.075833	2.0912	0.73484
500	0.574426	1.349766	1377158	0.126358	0.136522	1.881644	1.9002	0.97654
600	0.627959	1.687873	1721927	0.101258	0.176081	1.754932	1.7763	1.20295
700	0.671991	2.048699	2089790	0.083546	0.21465	1.667245	1.6913	1.42226
800	0.708645	2.432242	2480740	0.070448	0.252098	1.604066	1.6306	1.62727
900	0.739482	2.838504	2894767	0.060415	0.288413	1.557213	1.5861	1.82127
1000	0.76567	3.267484	3331864	0.052517	0.323632	1.52173	1.5528	2.00089

Table (4) provides details of the results for the element gold, which is considered the most obvious in terms of energy loss among heavy and high electron density elements, as the stopping power at low energy (10 MeV) recorded its lowest levels compared to the previous elements and equals

$18.02797 \mathrm{MeVcm}^2/\mathrm{g}$. This decrease is not due to weak absorption because the stopping power of gold is large due to its super density, but rather the reason is due to the low ratio of atomic number to atomic weight $\left(\frac{Z}{A} = 0.40\right)$ for gold compared to 0.50 for silicon. This reduces the number of electrons available for reaction per gram [3-9] in conjunction with the dominant effect of shell correction (C), which records a large jump at the starting energy of the falling proton and equals (18.09374). This large value compared to its appearances means physically that the greater proportion of electrons in the multiple shells of gold (K, L, M) are bound by a strong nuclear attraction and cannot participate at all in ionization processes due to the slow speed of the proton [7-8]. As the proton energy increases, we observe that the shell correction decays more slowly compared to silicon and copper, with a value of 0.65573 at 1000 MeV. The reason for this result is the strength of the atomic bonding energies of gold. At the same time, the density correction (δ) appears late and relatively late, as it begins to appear at the high energy of 900 MeV with a value of 0.16377946. Although gold is extremely dense, the logarithmic and physical conditions of the critical polarization limit ($X_0 = 0.2021$) and the large excitation potential of gold ($790\ eV$) delay the actual activation of the Sternheimer density effect correction limit compared to copper. This ultimately appears to be to finely adjust and direct the energy loss curve [5].

Table (4): Calculations of attenuation and energy loss of protons in the heavy metallic element (gold):

Proton kinetic energy (MeV)	Square of the proton's relativistic velocity β^2	Combined relativistic kinematic coefficient η^2	Maximum energy transfer in a single collision $W_{max}\ (eV)$	Correction value for the effect of the atomic shell C(unitless)	Density effect correction value δ(unitless)	Stopping Power $(\mathrm{MeV.cm}^2/\mathrm{g})$	Stopping Power $(\mathrm{MeV.cm}^2/\mathrm{g})$ Experiment [11]	Percentage Deviation %
10	0.02098	0.021429	21876.68	18.09374	0	18.02797	17.973	0.30584
50	0.098627	0.109419	111697.5	14.88694	0	5.82411	5.9079	1.41826
100	0.183351	0.224517	229179.4	8.421892	0	3.613603	3.6365	0.62963
150	0.256668	0.345295	352444.9	5.743565	0	2.76896	2.7811	0.43653
200	0.320538	0.471752	481493	4.303592	0	2.319556	2.3276	0.3456
300	0.42585	0.741705	756932.5	2.801098	0	1.851801	1.858	0.33362
400	0.508449	1.034376	1055490	2.031412	0	1.613861	1.6175	0.22501
500	0.574426	1.349766	1377158	1.567181	0	1.472649	1.4756	0.19996
600	0.627959	1.687873	1721927	1.258749	0	1.381197	1.3838	0.18814
700	0.671991	2.048699	2089790	1.040245	0	1.31862	1.321	0.18017
800	0.708645	2.432242	2480740	0.878194	0	1.274211	1.2764	0.17148
900	0.739482	2.838504	2894767	0.753805	0.16377946	1.228279	1.244	1.26378
1000	0.76567	3.267484	3331864	0.65573	0.177360155	1.203789	1.22	1.3288

When comparing the three tables (2,3,4) in a comprehensive manner, three physical facts emerge that explain the subtle differences in the mathematical results:

First: The effect of the shell correction (C)

We observe that the value of the shell correction increases progressively with increasing atomic number Z, as shown in Figure (1). For example, at an energy of 10 MeV, the shell correction limit for all elements is equal to

$$Si\ (1.293227) \Longrightarrow Cu\ (4.124163) \Longrightarrow Au\ (18.09374)$$

Figure (1) illustrates the quantum inertia of the inner orbital electrons, where the gold curve will show a large jump at the beginning, 18.09374, compared to silicon and copper. Then it shows how this effect diminishes and gradually fades away with increasing energy. This is because the greater

the positive charge of the nucleus (Z), the greater the binding strength of the inner orbital electrons to it, which is directly proportional to Z^2. Consequently, these electrons become unexcitable when protons collide at low energies. This inertia of the electrons requires us to introduce a large shell correction limit to subtract the contribution of these unexcited or unexcited electrons, which explains the lower stopping power of gold and copper compared to silicon at the same low energies [3-7].

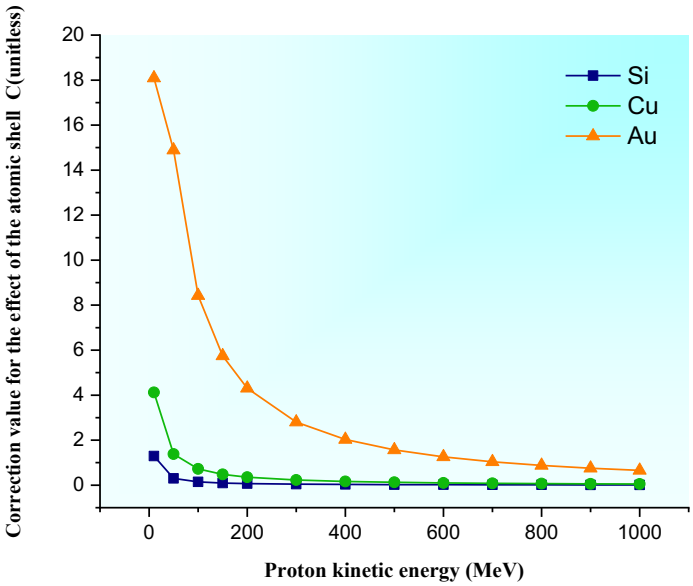

Figure (1): illustrates the relationship between the energy of the falling proton and the effect of the shell correction of the three elements.

Second: Behavior and activity of density correction (δ)

We observe from Figure (2) that there is a significant variation in the activation start energy and the density correction value at high energies:

A. In copper: Activation and density correction (δ) activity begin very early at 400 MeV and reach a high value (0.323632) at $1000\ MeV$.

B. In silicon: Activation is delayed until $900\ MeV$, reaching a final value of (0.15016).

C. In gold: Activation also begins late, at $900\ MeV$, reaching a final value of (0.177360155).

Figure (2) illustrates the density correction limit resulting from the polarization of the dense medium. Figure (2) clearly shows how the density correction limit in copper is activated early at 400 MeV due to the negative $(X_0 = -0.0254)$, while the activation in silicon and gold is delayed until $900\ MeV$.

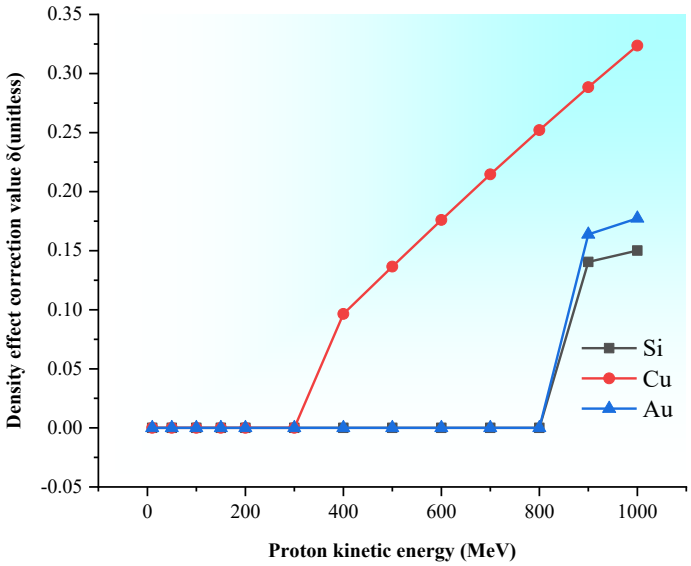

Figure (2): illustrates the relationship between the energy of the incident proton and the density correction activity of the three elements.

This indicates that the onset of density correction activation in the Sternheimer formula depends on the logical comparison condition based on the experimental limit X_0 and the excitation potential I, which means that the polarization of the metallic lattice of copper and its metallic bonding allow the onset of the density blocking process and the protection of distant electrons at much lower proton energies compared to gold and silicon, which have positive limits that require higher relative energies to activate the actual polarization of the medium [17-18].

Third: Direction of the total stopping power of a proton

At any constant kinetic energy of the proton, we always observe the following descending order of stopping power [9-10]:

$$Si\ \left(\frac{dE}{dx}\right) > Cu\ \left(\frac{dE}{dx}\right) > Au\ \left(\frac{dE}{dx}\right)$$

Figure (3) illustrates the stopping power of the proton and its inverse dependence on the atomic number at the same energy levels. We also observe the sharp drop in the curves at the beginning, followed by their stabilization at high energies.

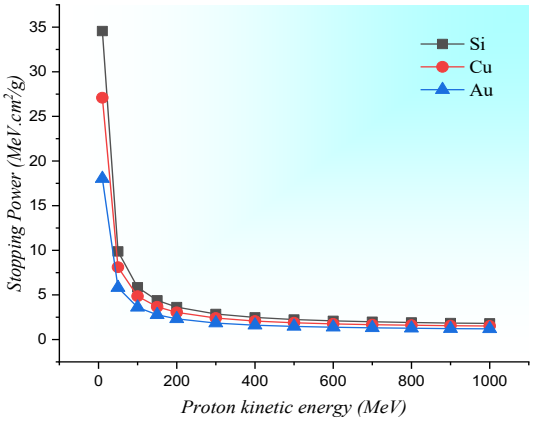

Figure (3): illustrates the relationship between the energy of the falling proton and the stopping power of the three elements.

This means that the stopping power represents the energy loss per gram of proton-absorbing material per square centimeter. Since heavy elements have a large atomic weight compared to their available electrons, and applying the $\frac{Z}{A}$ ratio, this decreases as the atomic number Z increases due to the increased number of neutrons in the nucleus to protect it from Coulomb repulsion, the number of electrons available for collision in one gram of gold is much less than in one gram of silicon. This electron decrease, supported by the strong binding force of the remaining internal electrons (shell correction), fully explains why the stopping power of light materials is much higher than that of heavy media in all incident particle energy ranges [3-5].

6. Conclusions

This study demonstrated that the mathematical modeling of stopping power cannot be reduced to simplified classical frameworks without incorporating the boundaries of comprehensive relativistic corrections. It was physically confirmed that the inverse relationship between atomic number and stopping power with increasing atomic number (Z) is primarily due to the decrease in the ratio of electrons available for interaction per gram, as applied by the $\left(\frac{Z}{A}\right)$ ratio. Furthermore, it was shown that shell correction (C) represents the dominant force in theoretical calculations at low energies, and its effect increases proportionally and strongly with increasing nuclear charge due to the strong bonding of electrons to it. Simultaneously, the effect of these atomic shells disappears entirely at high energies because the velocity of the incident proton exceeds the intrinsic orbital velocities of the bound electrons. On the other hand, the density correction limit (δ) appears as a control limit that prevents mathematical exaggeration in calculating the radioactive loss at relative energies approaching the speed of light, where the volumetric electron density of the metallic lattice, as is the case with copper, intervenes greatly in the process of initiating the activation of density shielding earlier compared to semiconductors and heavy elements such as gold. Thus, we confirm the conformity of the computational outputs with the international experimental tables and the success and integrity of the developed and proposed Beth-Bloch equation in simulating the radioactive reaction with extreme accuracy and the lowest error rate.

7. References

1. Knoll, Glenn F. *Radiation detection and measurement*. John Wiley & Sons, 2010.
2. Turner, James E. *Atoms, radiation, and radiation protection*. John Wiley & Sons, 2008.
3. Evans, Robley Dunglison, and R. D. Evans. *The atomic nucleus*. Vol. 582. New York: McGraw-Hill, 1955.
4. Krane, Kenneth S. *Introductory nuclear physics*. John Wiley & Sons, 1991..
5. Leo, William R. "Techniques for nuclear and particle physics experiments." *Nucl Instrum Methods Phys Res* 834 (1988): 290
6. Ziegler, James F., Matthias D. Ziegler, and Jochen P. Biersack. "SRIM–The stopping and range of ions in matter (2010)." *Nuclear Instruments and Methods in Physics Research Section B: Beam Interactions with Materials and Atoms* 268.11-12 (2010): 1818-1823.
7. Bohr, Niels. "II. On the theory of the decrease of velocity of moving electrified particles on passing through matter." *The London, Edinburgh, and Dublin Philosophical Magazine and Journal of Science* 25.145 (1913): 10-31.
8. Fano, U. "Penetration of protons, alpha particles, and mesons." *Annual Review of Nuclear Science* 13.1 (1963): 1-66..
9. ICRU Report 49, *Stopping Powers and Ranges for Protons and Alpha Particles*. International Commission on Radiation Units and Measurements, Bethesda, MD(1993).
10. Berger, Martin J., and Stephen M. Seltzer. "Stopping powers and ranges of electrons and positrons." *Unknown* (1982)..

11. Janni, Joseph F. "Proton range-energy tables, 1 keV-10 GeV, energy loss, range, path length, time-of-flight, straggling, multiple scattering, and nuclear interaction probability. Part I. For 63 compounds." *Atomic data and nuclear data tables* 27 (1982): 147.
12. Ziegler, James F., and Jochen P. Biersack. "The stopping and range of ions in matter." *Treatise on heavy-ion science: volume 6: astrophysics, chemistry, and condensed matter*. Boston, MA: Springer US, 1985. 93-129.
13. Merzbacher, Eugen. *Quantum mechanics*. John Wiley & Sons, 1998..
14. Jackson, John David. "Classical electrodynamics 3rd ed john wiley & sons." *Inc., NewYork, NY* (1999): 5..
15. Karshenboim, Savely G. "Adjusted recommended values of the fundamental physical constants: An overview of the data and results of the CODATA-2006 adjustment." *The European Physical Journal Special Topics* 172.1 (2009): 385-397..
16. Mohr, Peter J., and Barry N. Taylor. "CODATA recommended values of the fundamental physical constants: 2002." *Reviews of modern physics* 77.1 (2005): 1-107.
17. Sternheimer, Rudolph M. "The density effect for the ionization loss in various materials." *Physical Review* 88.4 (1952): 851.
18. Sternheimer, R. M., S. M. Seltzer, and M. J. Berger. "Density effect for the ionization loss of charged particles in various substances." *Physical review B* 26.11 (1982): 6067.